

RSC Advances



This is an *Accepted Manuscript*, which has been through the Royal Society of Chemistry peer review process and has been accepted for publication.

Accepted Manuscripts are published online shortly after acceptance, before technical editing, formatting and proof reading. Using this free service, authors can make their results available to the community, in citable form, before we publish the edited article. This *Accepted Manuscript* will be replaced by the edited, formatted and paginated article as soon as this is available.

You can find more information about *Accepted Manuscripts* in the [Information for Authors](#).

Please note that technical editing may introduce minor changes to the text and/or graphics, which may alter content. The journal's standard [Terms & Conditions](#) and the [Ethical guidelines](#) still apply. In no event shall the Royal Society of Chemistry be held responsible for any errors or omissions in this *Accepted Manuscript* or any consequences arising from the use of any information it contains.

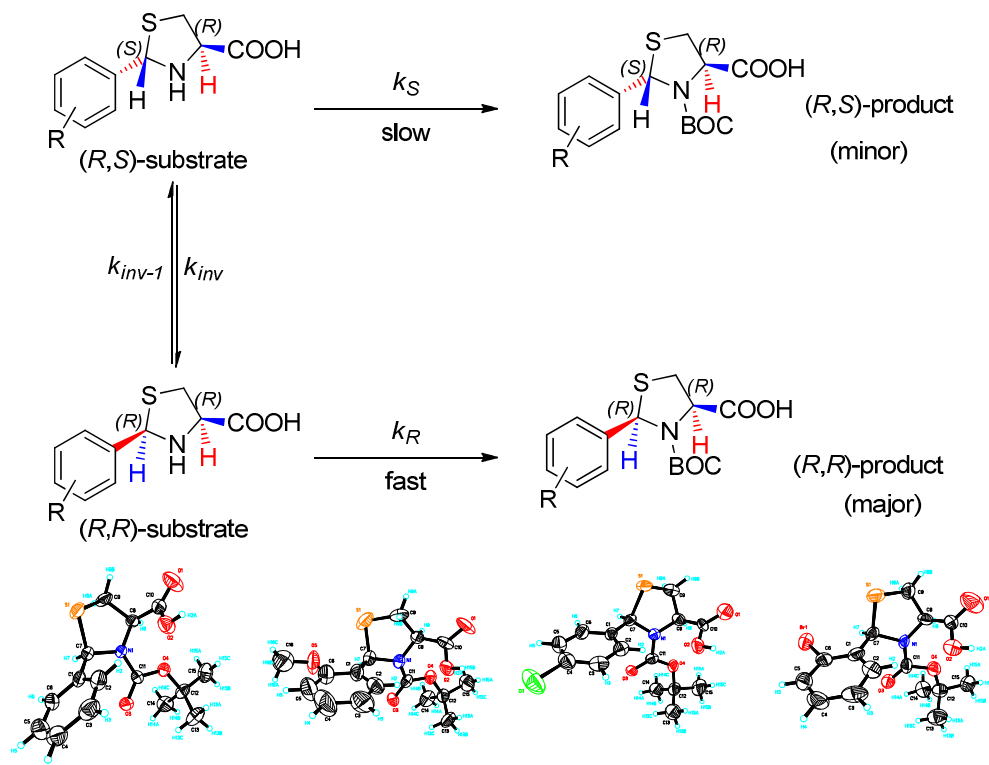
Synthesis, Characterization and Antibacterial Activities of *N*-*tert*-Butoxycarbonyl-Thiazolidine Carboxylic Acid

Zhong-Cheng Song^{a,b}, Gao-Yuan Ma^b and Hai-Liang Zhu^{a,b*}

^a School of Life Sciences, Zhejiang Chinese Medical University, Hangzhou, Zhejiang, P. R. China, 310053

^b School of Life Sciences, Nanjing University, Nanjing, Jiangsu, P. R. China, 210093

*Corresponding Author, E-mail: zhuhl@nju.edu.cn; Fax: +86-25-83592672; Tel: +86-25-83592672



The mechanism of dynamic kinetic resolution by the formation of *N*-Boc-TCAs was proposed and a qualitative explanation was interpreted according to Curtin-Hammett principle. Such a mechanism of action of a nucleophilic substitution reaction through an intramolecular hydrogen bonding could be widely applied in the organic syntheses of particular enantiomer.

Cite this: DOI: 10.1039/c0xx00000x

www.rsc.org/xxxxxx

ARTICLE TYPE

Synthesis, Characterization and Antibacterial Activities of *N-tert*-Butoxycarbonyl-Thiazolidine Carboxylic Acid

Zhong-Cheng Song^{a,b}, Gao-Yuan Ma^b and Hai-Liang Zhu^{a, b*}

^a School of Life Sciences, Zhejiang Chinese Medical University, Hangzhou, Zhejiang, P. R. China, 310053

^b School of Life Sciences, Nanjing University, Nanjing, Jiangsu, P. R. China, 210093

*Corresponding Author, E-mail: zhuhl@nju.edu.cn; Fax: +86-25- 83592672; Tel: +86-25-83592672

Received (in XXX, XXX) Xth XXXXXXXXX 20XX, Accepted Xth XXXXXXXXX 20XX

DOI: 10.1039/b000000x

A possible mechanism of dynamic kinetic resolution by the formation of *N-tert*-butoxycarbonyl-thiazolidine carboxylic acid was proposed and validated by a quantitative density functional theoretical calculation according to Curtin-Hammett principle. Such a mechanism of action of a nucleophilic substitution reaction through an intramolecular hydrogen bonding could be widely applied in the organic syntheses of particular enantiomer. Antibacterial activities showed that most of the *N-tert*-butoxycarbonyl-(2*R*)-arylthiazolidine-(4*R*)-carboxylic acid derivatives exhibited better antibacterial activities against the four bacterial strains than related (2*R*)-arylthiazolidine-(4*R*)-carboxylic acid derivatives.

1 Introduction

Kinetic resolution has long been recognized as an effective tool for the preparation of enantiomerically pure compounds for fine chemicals (i.e. agrochemicals and pharmaceuticals) and material science (i.e. liquid crystals and polymers)¹⁻². However, the main drawback of the conventional kinetic resolution was that the obtained maximum theoretical yield of one stereoisomer of the starting material or product could be 50%, which was too low to allow a positive economic and environmental balance for such transformations³. To overcome this limitation, of all the strategies that allow the transformation of both enantiomers of a racemate into a single enantiomer of the product, dynamic kinetic resolution (DKR) has been the focus of many studies in recent years. With DKR, the reactant isomers must be in rapid equilibrium, making removal of one isomer the rate determining step, and the product could be obtained optically pure in 100% yield (Figure 1)⁴⁻⁵.

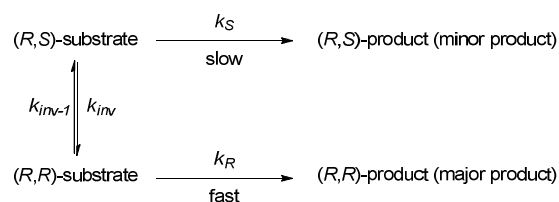


Figure 1. Schematic representation of a dynamic kinetic resolution (DKR).

The steric course of the reaction between L-cysteine and aldehydes deserved much attention because this reaction had been implicated in several biochemical processes⁶⁻⁸. An analogous condensation reaction constituted the first step in the syntheses of

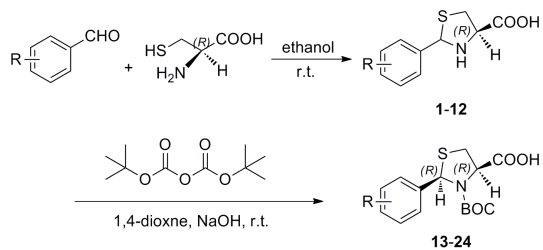
important natural products, such as penicillin and biotin⁹⁻¹⁰. Therefore, thiazolidine derivatives have become especially noteworthy in recent years¹¹⁻¹³.

In this paper, because of the wide application of the *tert*-butoxycarbonyl(Boc) protecting group, under the guidance of the Curtin-Hammett principle, we synthesized a series of *N*-Boc-(2*R*)-aryl-thiazolidine-(4*R*)-carboxylic acids (*N*-Boc-TCAs) compounds using the control factors of intramolecular hydrogen bond induced-steric-hindrance, combined with dynamic kinetic resolution¹⁴⁻¹⁸. The corresponding reaction mechanism and the corresponding theoretical explanation were proposed. In order to compare the differences of antibacterial activities of *N*-Boc-TCAs and TCAs, we tested the antibacterial activities of them against the four bacteria, Grampositive (*Bacillus subtilis* ATCC 6633 and *Staphylococcus aureus* ATCC 6538) and Gram-negative (*Pseudomonas aeruginosa* ATCC 13525 and *Escherichia coli* ATCC 35218), which often caused infection in burned patients.

2 Results and Discussion

2.1 Chemistry

The synthetic route to *N*-Boc-TCAs (**13-24**) is shown in Scheme 1. The syntheses of TCAs (**1-12**) were carried out using our previous literature method¹⁶, by reaction of commercially available aromatic aldehyde and L-cysteine in the presence of ethanol with excellent yield. Treatment of **1-12** with *t*-butyloxycarbonyl anhydride ((Boc)₂O) yielded *N*-Boc-TCAs (**13-24**)¹⁶. The structures of the synthesized compounds (**1-24**) were listed in Table 1. All of the synthetic compounds were characterized by spectroscopic data, which were full accordance with their structures.



Scheme 1. Syntheses of 2-aryl-*N*-Boc-1,3-thiazolidine acid (TCAs) **13-24**.

Table 1. The structures of the synthesized compounds (**1-24**)

		1-12					13-24						
Compounds		R ₁	R ₂	R ₃	R ₄	R ₅	Compounds		R ₁	R ₂	R ₃	R ₄	R ₅
1	13	H	H	H	H	H	13	H	H	H	H	H	H
2	14	H	H	OH	H	H	14	H	H	OH	H	H	H
3	15	OMe	H	H	H	H	15	OMe	H	H	H	H	H
4	16	H	H	OMe	H	H	16	H	H	OMe	H	H	H
5	17	H	F	H	H	H	17	H	F	H	H	H	H
6	18	H	H	F	H	H	18	H	H	F	H	H	H
7	19	Cl	H	H	H	H	19	Cl	H	H	H	H	H
8	20	H	Cl	H	H	H	20	H	Cl	H	H	H	H
9	21	H	H	Cl	H	H	21	H	H	Cl	H	H	H
10	22	Br	H	H	H	H	22	Br	H	H	H	H	H
11	23	H	H	Br	H	H	23	H	H	Br	H	H	H
12	24	OH	H	H	H	H	24	OH	H	H	H	H	H

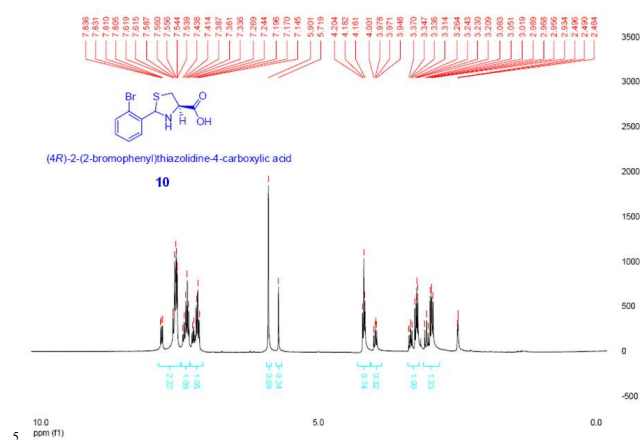


Figure 2. ¹H NMR of the compound **10**

From the ¹H NMR results, the unprotected TCA compounds 2-aryl-1,3-thiazolidine acids were obtained two diastereomers. The ratio of the most two diastereomers is nearly to 1:1. For example, from the **Figure 2** and **Figure 3**, the ¹H NMR of the new born 4-position H (CH) of the thiazolidine ring in the compound **10** has two peaks and the chemical shift values are 5.90 and 5.72. However, the ¹H NMR of the 4-position H (CH) of the thiazolidine ring in the compound **22** only has one single peak and the chemical shift value is 6.12. It suggested that the unprotected TCA compounds 2-aryl-1,3-thiazolidine acids have two diastereomers and the protected TCA compound 2-aryl-*N*-Boc-1,3-thiazolidine acid is single chiral isomer.

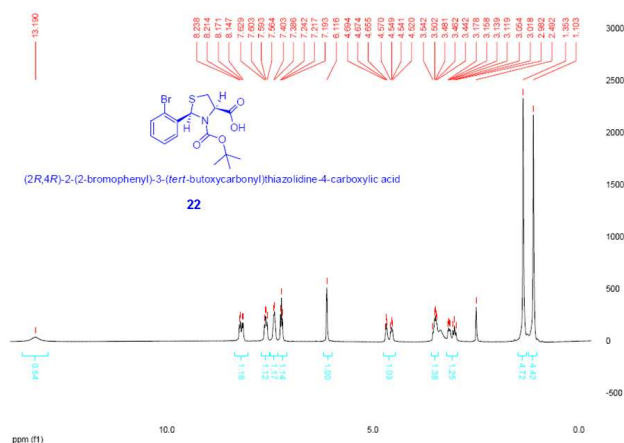


Figure 3. ¹H NMR of the compound **22**

2.2 Crystal structure Analysis

In order to study the absolute structure of the product, we cultured some of the crystal structure of *N*-BOC-TCAs which are helpful to explain the mechanism of formation of *N*-BOC-TCAs. Fortunately, X-ray single-crystal diffraction data for compounds **13**, **15**, **21** and **22** were collected on a Nonius CAD4 diffractometer equipped with graphite-monochromatized MoK α radiation. **Table 2.** selected bond lengths (Å), bond angles (°) and torsion angles(°) for compounds **13**, **15**, **21** and **22**.

	13	15	21	22
H(7)--- H(8) ^{#1}	3.418	3.550	3.456	3.481
H(7)--- C(10) ^{#1}	4.227	4.447	4.247	4.278
H(8)--- C(6) ^{#1}	4.444	4.262	4.444	4.397
N(1)-C(7)-C(6)	116.5	116.2	117.2	112.9
N(1)-C(7)-S(1)	103.5	103.3	102.2	107.6
C(6)-C(7)-S(1)	110.8	113.6	109.2	101.9
C(6)-C(7)-H(7)	108.6	107.8	109.3	111.3
N(1)-C(7)- H(7)	108.6	107.8	109.3	111.3
S(1)-C(7)- H(7)	108.6	107.8	109.3	111.3
N(1)-C(8)-C(9)	105.7	105.5	106.6	106.1
N(1)-C(8)-C(10)	114.2	114.0	115.7	113.3
C(9)-C(8)-C(10)	111.1	109.7	109.6	118.3
C(9)-C(8)-H(8)	108.6	109.2	108.2	106.1
N(1)-C(8)- H(8)	108.6	109.2	108.2	106.1
C(10)-C(8)- H(8)	108.6	109.2	108.2	106.1
Φ_1 [C(1)-C(2)-C(3)-C(4)-C(5)-C(6)] ^{#2}	0.0059	0.0049	0.0052	0.0097
Φ_2 [C(7)-N(1)-C(8)-C(9)-S(1)] ^{#2}	0.2078	0.2003	0.1972	0.2035
$\Phi_1 \cap \Phi_2$ ^{#3}	98.8	101.2	77.2	69.6

^{#1} represents the calculate value of space distance; ^{#2} represents the mean deviation distances from the surface; ^{#3} represents the dihedral angle of two ring surfaces Φ_1 and Φ_2 .

($\lambda = 0.71073$ Å) radiation. The program CAD4 software was used for data collection and cell refinement. Data reduction was solved by XCAD4 program. Structure was solved by direct

methods using the SHELXS program of the SHELXTL package and refined by full-matrix least-squares methods with SHELXL¹⁹.

The selected bond distances, bond angles and torsion angles are given in **Table 2**. Crystal structure data of compounds **13**, **15**, **21** and **22** are given in **Table 3**. **Figure 4**, **Figure 5**, **Figure 6** and **Figure 7** gave typically perspective view of compounds **13**, **15**, **21** and **22** with the atomic labeling system, respectively. Further details of the crystal structure investigations may be obtained from the Fachinformationszentrum Karlsruhe, 76344 Eggenstein-Leopoldshafen, Germany (fax: (+49) 7247-808-666; e-mail: crysdata@fiz-karlsruhe.de) on quoting the deposition numbers CSD-760948, -703635, -703637, and -703638.

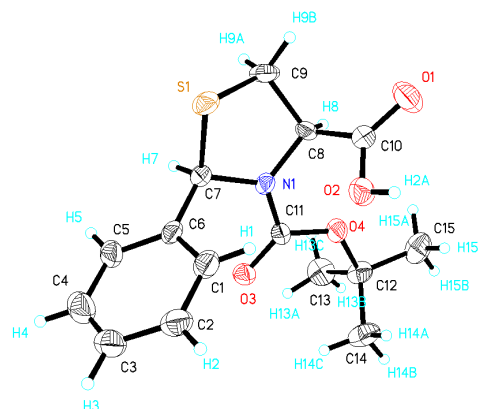


Figure 4. Molecular structure (thermal ellipsoids at the 35% probability level) of compound **13**.

Table 3. Crystal structure data of compounds **13**, **15**, **21** and **22**.

Compound	13	15	21	22
Formula	C ₁₅ H ₁₉ NO ₄ S	C ₁₆ H ₂₁ NO ₅ S	C ₁₅ H ₁₈ ClNO ₄ S	C ₁₅ H ₁₈ BrNO ₄ S
<i>Mr</i>	309.37	339.40	343.81	388.27
Crystal size (mm ³)	0.30×0.20×0.10	0.30×0.20×0.10	0.30×0.20×0.10	0.20×0.10×0.10
Crystal system	Monoclinic	Orthorhombic	Monoclinic	Monoclinic
Space group	<i>P</i> 2 ₁	<i>P</i> 2 ₁ 2 ₁ 2 ₁	<i>P</i> 2 ₁	<i>P</i> 2 ₁
<i>a</i> (Å)	10.308(2)	6.4240(13)	6.4600(13)	10.485(2)
<i>b</i> (Å)	6.3790(13)	10.255(2)	10.641(2)	6.6020(13)
<i>c</i> (Å)	12.174(2)	27.064(5)	12.411(3)	12.803(3)
α (°C)	90.00	90.00	90.00	90.00
β (°C)	100.71(3)	90.00	94.52(3)	103.81(3)
γ (°C)	90.00	90.00	90.00	90.00
<i>V</i> (Å ³)	786.6(3)	1782.9(6)	850.5(3)	860.6(3)
<i>Z</i>	2	4	2	2
<i>D_c</i> (g/cm ³)	1.306	1.264	1.343	1.498
μ (mm ⁻¹)	0.220	0.204	0.363	2.525
<i>F</i> (000)	328	720	360	396
θ range (°)	1.70/25.26	1.50/25.16	1.65 / 25.26	1.64/ 25.16
Index range (<i>h, k, l</i>)	-12/12, 0/7, 0/14	0/7, 0/12, 0/32	-7/7, 0/12, 0/14	-12/12, 0/7, 0/15
Reflections collected / unique	1660 / 1571	1887 / 1648	1638 / 1462	1687 / 1459
<i>R</i> (<i>int</i>)	0.0406	0.0248	0.0461	0.0362
Observed reflections <i>I</i> >2 σ (<i>I</i>)	1348	1317	1363	1281
Min. and max. transmission	0.9783 and 0.9369	0.9798 and 0.9412	0.9646 and 0.8989	0.7863 and 0.6321
Data/restraints/parameters	1571 / 49 / 190	1887/ 43 / 207	1638 / 78 / 185	1687 / 61 / 203
Goodness-of-fit on <i>F</i> ²	1.005	1.092	1.084	1.036
<i>R_i</i> , <i>wR₂</i> [<i>I</i> >2 σ (<i>I</i>)]	0.0524/0.1273	0.0726/0.1909	0.0619 / 0.1453	0.0525/0.1233
<i>R₁</i> , <i>wR₂</i>	0.0674/0.1558	0.0998/0.2200	0.0761 / 0.1592	0.0728/0.1363
Absolute structure parameter	0.0(2)	0.1(3)	-0.09(19)	-0.02(2)
Large diff. peak and hole (e Å ⁻³)	0.354/-0.228	0.428 / -0.387	0.435 / -0.368	0.383 and -0.480

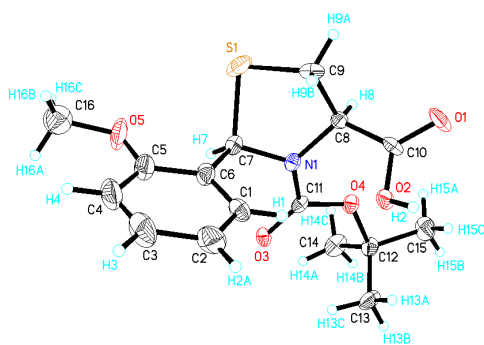


Figure 5. Molecular structure (thermal ellipsoids at the 35% probability level) of compound **15**.

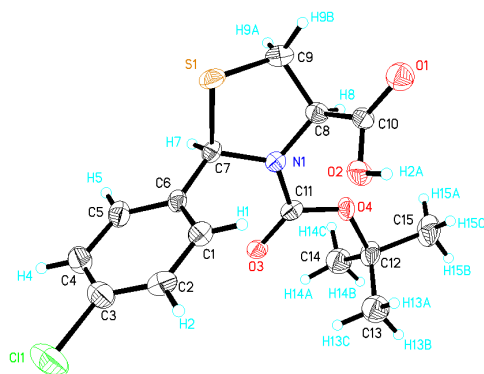


Figure 6. Molecular structure (thermal ellipsoids at the 35% probability level) of compound **21**.

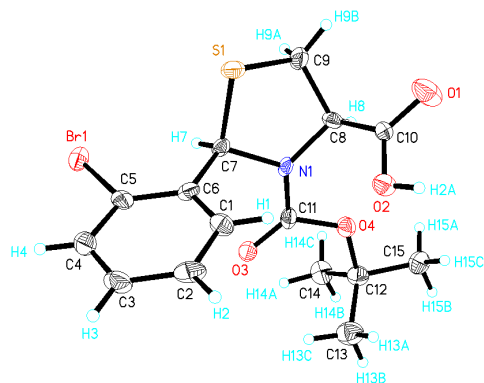


Figure 7. Molecular structure (thermal ellipsoids at the 35% probability level) of compound **22**.

From **Table 2** and **Figure 4**, for compound **13**, we

could see that the surface mean deviation angles of benzene ring C1-C2-C3-C4-C5-C6 defined as Φ_1 and ring C7-N1-C8-C9-S1 defined as Φ_2 were 0.0060 Å and 0.2079 Å respectively. In addition, the dihedral angle of surfaces Φ_1 and Φ_2 was 98.8°, demonstrating that the two surfaces were almost in a vertical position, which arranged in the structure of stable conformations, avoiding a large steric effect of the substituents between the benzene ring and the newly formed five-membered ring. The space distance length of H7---H8 was 3.418 Å by calculating value, while that of H7---C10 was 4.227 Å, which showed that the space distance length of the latter is longer than that of the former, therefore, atom H7 and atom C10 were indicated in the opposite position of ring Φ_2 . By comparing the bond angles with C7 and C8 as the centers (see **Table 2**), every bond angle was almost near to 109.5°, which demonstrated that C7 and C8 were sp^3 -hybrid. Because of H7 and C10 on both side of ring Φ_2 , H7 and H8 were on same side of ring Φ_2 . From the starting structure of compound L-cysteine, the configuration of C8 of compound **13** was (*R*)-configuration. Therefore, the configuration of C7 of compound **13** also was (*R*)-configuration according to IUPAC nomenclature. Furthermore, from **Table 3**, we can see that the Flack parameter of crystal **13** is 0.0(2). Consequently to literature, compound **13** can be showed a (*2R,4R*)-configuration as a single chiral isomer.²⁰⁻²² Likewise, from **Table 3**, **Figure 5**, **Figure 6** and **Figure 7**, the crystal structures of the other three compounds **15**, **21** and **22** were analyzed based on the same consideration. The result is that compounds **15**, **21** and **22** is (*2R,4R*)-configuration as a single chiral isomer respectively.

2.3 Mechanism of reaction

To study the cause of the single chiral isomer, we referred corresponding mechanism of reaction of *N*-Boc-TCAs. As showed in **Figure 8**, the reaction of (*R*)-cysteine and aryl aldehyde produced the Schiff base intermediate **I**, which had two epimers (*Z*)-**II** and (*E*)-**II**. (*2S,4R*)-**III** and (*2R,4R*)-**III** were generated through intramolecular hydrogen bond activation respectively. (*2S,4R*)-**III** and (*2R,4R*)-**III** were alkalinized and then (*2S,4R*)-**IV** and (*2R,4R*)-**IV** were also formed through intramolecular hydrogen bonding, respectively. Theoretically, (*2S,4R*)-**V** and (*2R,4R*)-**V** should be rapidly equilibrated into an approximately 1:1 mixture like (*2S,4R*)-**III** and (*2R,4R*)-**III**. However, one pair of electrons of N atom of (*2S,4R*)-**IV** or (*2R,4R*)-**IV** attacked C atom of the carbonyl of *di-tert*-butyl carbonate through an S_N2 substitution reaction. This N atom was also a fictitious chiral center. Because of sterical intramolecular hydrogen bond activation, one pair of electrons of N atom of (*2S,4R*)-**IV** or (*2R,4R*)-**IV** must assault C atom of the carbonyl of *di-tert*-butyl carbonate from the back of the ring Φ_2 . Nevertheless, the sterically

crowded effect of suprafacial aryl of **(2S,4R)-IV** was larger than that of different aryl surface of **(2R,4R)-IV**. Obviously, the rate of step **(2R,4R)-IV** \rightarrow **(2R,4R)-V** should be much faster than that of step **(2S,4R)-IV** \rightarrow **(2S,4R)-V** and the rate constants named k_2 and k_1 respectively. So, k_2 was much larger than k_1 ($k_2 \gg k_1$). Because all the reactions were synthesized at room temperature, the reaction rate was assumed to be controlled by dynamic kinetic resolution effect. Therefore, the reaction rate of **(2S,4R)-V** \rightarrow **(2S,4R)-IV** \rightarrow **(2S,4R)-III** \rightarrow **(Z)-II** \rightarrow Schiff base intermediate **I** \rightarrow **(E)-II** \rightarrow **(2R,4R)-III** \rightarrow **(2R,4R)-IV** \rightarrow **(2R,4R)-V** should be much faster than that of inverse sequence. As a result, **(2S,4R)-V** was almost converted into **(2R,4R)-V**. As acquired, **(2R)**-aryl-3-*tert*-butoxycarbonyl-1,3-thiazolidine-

(4R)-carboxylic acid as the single product was obtained because of dynamic kinetic resolution effect. A corresponding qualitative explanation from the theory was interpreted according to dynamic kinetic resolution and Curtin-Hammett principle combined with above reaction mechanism, see **Figure 9**⁴⁻⁵. At first, we found the potential energy was very low in the transformation process of intermediate **(2S,4R)-IV** \leftrightarrow **(2S,4R)-III** \leftrightarrow **(Z)-II** \leftrightarrow Schiff base intermediate **I** \leftrightarrow **(E)-II** \leftrightarrow **(2R,4R)-III** \leftrightarrow **(2R,4R)-IV** (**Figure 8** and **Figure 9**). So, the above transformation process could be simplified **(2S,4R)-IV** \leftrightarrow **(2R,4R)-IV** (**Figure 10**).

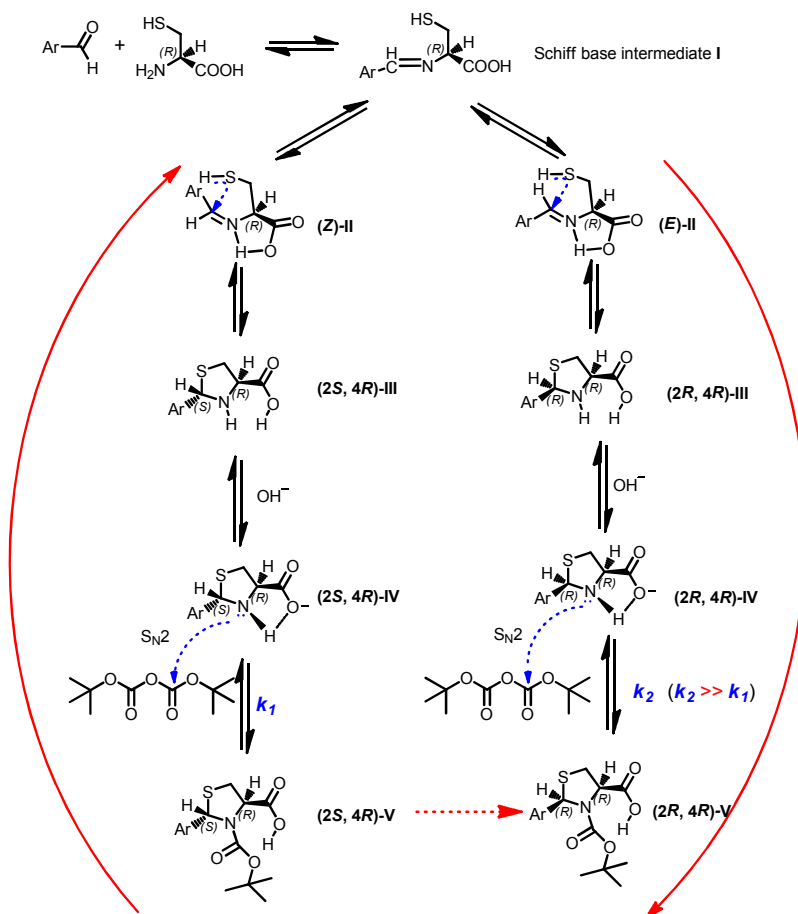


Figure 8. The proposed mechanism of formation of compounds 13-24.

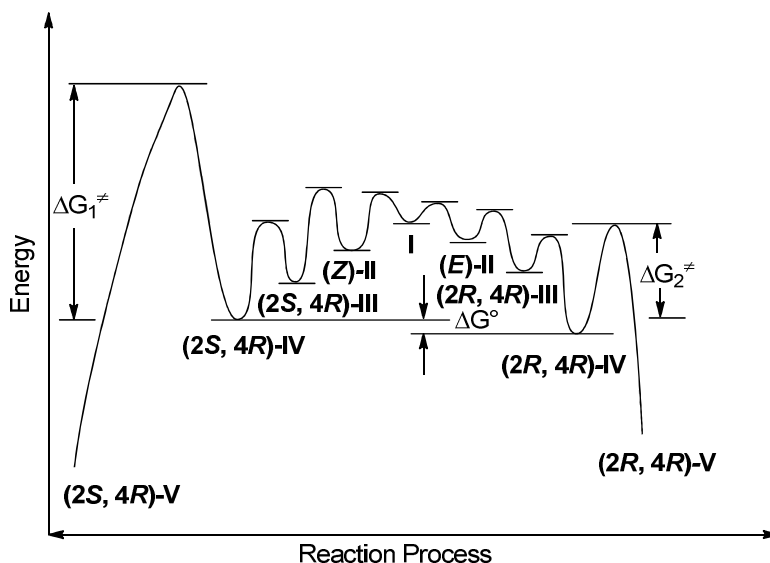


Figure 9. Curtin-Hammett mechanism of 2-aryl-*N*-Boc-1,3-thiazolidine derivatives. ΔG_1^\ddagger represents the Gibbs free potential energy of $(2S, 4R)\text{-IV} \rightarrow (2S, 4R)\text{-V}$, ΔG_2^\ddagger represents the Gibbs free potential energy of $(2R, 4R)\text{-IV} \rightarrow (2R, 4R)\text{-V}$; ΔG° represents the Gibbs free potential energy of $(2S, 4R)\text{-IV} \rightarrow (2R, 4R)\text{-IV}$.

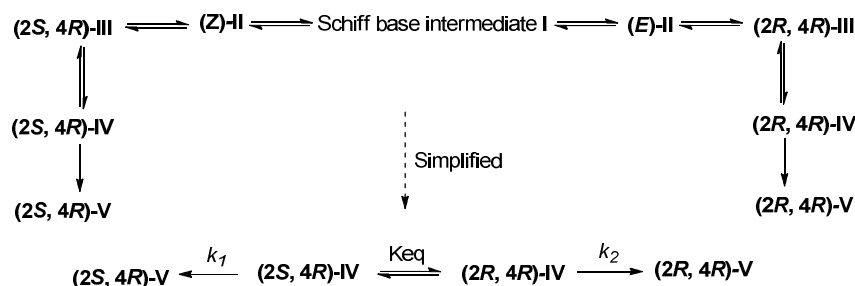


Figure 10. Simplified reaction mechanism of 2-aryl-*N*-Boc-1,3-thiazolidine derivatives

According to the relationship between equilibrium constant and Gibbs free energy, we can get **Equation 1**:

$$\frac{[\text{cis-V}]}{[\text{trans-V}]} = \frac{k_2}{k_1} K_{\text{eq}} = \frac{e^{-\Delta G_2^\ddagger/RT}}{e^{-\Delta G_1^\ddagger/RT}} (e^{-\Delta G^\circ/RT})$$

$$= e^{-(\Delta G_2^\ddagger + \Delta G^\circ - \Delta G_1^\ddagger)/RT}$$

Equation 1

Equation 1. The relationship between equilibrium constant and Gibbs free energy.

In the theoretical model, the Ar group was simplified to Ph, and the $(\text{Boc})_2\text{O}$ was simplified to $(\text{MeOCO})_2\text{O}$. All calculations were performed by Gaussian03²³ software suite. Geometries of intermediates and transition states were fully optimized without any constraints using B3LYP²⁴⁻²⁵ functional with 6-31+G(d) basis set. All geometries were confirmed by frequency analysis in which an intermediate has no negative frequency and a transition state has only one negative frequency corresponding to the reaction coordinate. The thermodynamic corrections for Gibbs free energy at 298.15 K were calculated at the same level of geometrical optimizations. Single point calculations were conducted using B3LYP functional with a larger basis set, 6-311+G(2d,p). The solvent

effects were addressed by the polarizable continuum model using the integral equation formalism variant (IEFPCM) with UAHF radii²⁶. The structures of transition state are depicted in **Figure 11** and **Figure 12**.

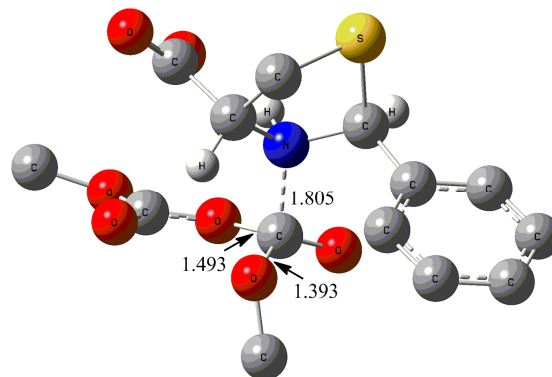


Figure 11. The structure of transition state leading to $(2S, 4R)\text{-V}$. Key bond lengths were shown in the unit of Angstrom.

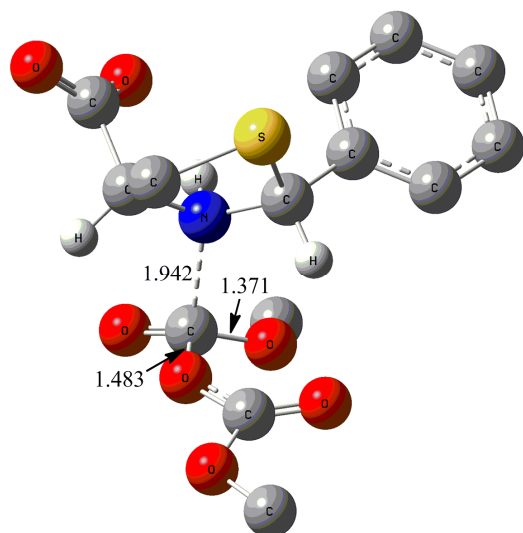


Figure 12. The structure of transition state leading to **(2R,4R)-V**. Key bond lengths were shown in the unit of Angstrom.

According to the calculate results, ΔG_1^\ddagger , ΔG_2^\ddagger and ΔG^0 were 174.7 kJ/mol, 149.5 kJ/mol and 3.3 kJ/mol, respectively. All data were substituted to **Equation 1**, and the value of $[(2R,4R)-V]/[(2S,4R)-V]$ was 6705. The percentage of **(2R,4R)-V** accounted the entire system (**(2R,4R)-V** and **(2S,4R)-V**) of 99.99%.

Therefore, the yield of **(2R,4R)-V** is much more than that of **(2S,4R)-V** in the case of such high steric hindrance potential energy. As the above analysis, the single chiral isomer 2-aryl-*N*-Boc-thiazolidine derivatives were gained under the control factors of intramolecular hydrogen bond induced-steric-hindrance.

2.4 In vitro antibacterial assay

The activities of synthesized *N*-Boc-TCAs were tested against Grampositive (*Bacillus subtilis* ATCC 6633 (*B. subtilis*) and *Staphylococcus aureus* ATCC 6538 (*S. aureus*)) and Gram-negative (*Pseudomonas aeruginosa* ATCC 13525 (*P. aeruginosa*) and *Escherichia coli* ATCC 35218 (*E. coli*)), which often caused infection in burned patients by MTT method. The IC_{50} s of the compounds against four bacteria are presented in **Table 4**. Also included are the activities of reference compounds Kanamycin G and Penicillin B. Antibacterial activities showed that most of the *N*-Boc-TCAs exhibited better antibacterial activities against the four bacterial strains than relative TCAs.

3 Conclusions

In summary, the mechanism of dynamic kinetic resolution by the formation of *N*-Boc-TCAs was proposed and a quantitative theoretical calculation was interpreted by Gaussian03 software suite according

to Curtin-Hammett principle. Such a mechanism of anucleophilic substitution reaction through an intramolecular hydrogen bonding could be widely applied in the organic syntheses of special enantiomers. Antibacterial activities showed that most of the *N*-Boc-TCAs exhibited better antibacterial activities against Grampositive bacteria(*B. subtilis* and *S. aureus*) and Gram-negative bacteria(*P. aeruginosa* and *E. coli*) than relative TCAs.

Table 4. IC_{50} values of the synthesized TCAs **1-12** and *N*-Boc-TCAs **13-24** against the four bacteria.

Compound	IC_{50} s(μ g/mL)			
	Gram positive		Gram negative	
	<i>B. subtilis</i>	<i>S. aureus</i>	<i>P. aeruginosa</i>	<i>E. coli</i>
1	3.125	12.5	>50	25
2	25	>50	25	>50
3	6.25	12.5	12.5	6.25
4	12.5	25	>50	>50
5	3.125	6.25	1.562	6.25
6	6.25	12.5	3.125	25
7	12.5	12.5	12.5	25
8	6.25	12.5	6.25	12.5
9	12.5	12.5	12.5	50
10	25	25	25	50
11	25	25	12.5	25
12	3.125	6.25	1.562	12.5
13	3.125	0.78	0.78	0.39
14	0.39	3.125	0.39	0.78
15	1.562	1.562	0.78	0.39
16	3.125	1.562	0.39	0.78
17	0.39	0.39	0.195	1.562
18	1.562	0.78	0.78	1.562
19	1.562	1.562	0.78	0.78
20	0.78	0.78	0.39	0.39
21	1.562	0.78	0.78	1.562
22	1.562	3.125	0.78	1.562
23	3.125	3.125	0.39	0.39
24	0.39	0.39	0.195	0.78
Kanamycin G	0.39	1.562	3.125	3.125
Penicillin B	1.562	1.562	6.25	6.25

4 Experimental Section

4.1 Chemistry

All the reagents and solvents used were analytical reagent grade or were purified by standard methods before use. ESI mass spectra were obtained on a Mariner System 5304 mass spectrometer, and ^1H NMR was recorded at DPX300 in DMSO- d_6 or CDCl_3 on a Bruker spectrometer. Elemental analyses were performed on a CHN-O-Rapid instrument and were within $\pm 0.4\%$ of the theoretical values.

General Procedure for the Preparation of TCA derivatives 1-12. A mixture of L-cysteine (0.121 g, 1.0 mmol) and appropriate aldehyde (1.0 mmol) in ethanol (25 mL) was stirred at room temperature for 8 h, and the solid separated was collected, washed with diethyl ether and dried to obtain 1-12.

4.1.1 (4R)-2-phenylthiazolidine-4-carboxylic acid (1) yield 84%. ^1H NMR(300 MHz, DMSO- d_6) δ 7.53-7.24 (m, 5H), 5.68 (s, 0.5H), 5.50 (s, 0.5H), 4.26-4.22 (m, 0.5H), 3.93-3.88 (m, 0.5H), 3.41-3.27 (m, 1H), 3.17-3.05 (m, 1H). MS (ESI) m/z 210 (M+1). Anal. Calcd for $\text{C}_{10}\text{H}_{11}\text{NO}_2\text{S}$: C, 57.39; H, 5.30; N, 6.69. Found: C, 57.62; H, 5.28; N, 6.71.

4.1.2

(4R)-2-(4-hydroxyphenyl)thiazolidine-4-carboxylic acid (2) yield 87%. ^1H NMR(300 MHz, DMSO- d_6) δ 7.32-7.23 (m, 2H), 6.75-6.69 (m, 2H), 5.53 (s, 0.5H), 5.39 (s, 0.5H), 4.27-4.23 (m, 0.5H), 3.86-3.81 (m, 0.5H), 3.37-3.24 (m, 1H), 3.17-3.01 (m, 1H). MS (ESI) m/z 226 (M+1). Anal. Calcd for $\text{C}_{10}\text{H}_{11}\text{NO}_3\text{S}$: C, 53.32; H, 4.92; N, 6.22. Found: C, 53.50; H, 4.94; N, 6.20.

4.1.3

(4R)-2-(2-methoxyphenyl)thiazolidine-4-carboxylic acid (3) yield 82%. ^1H NMR(300 MHz, DMSO- d_6) δ 7.51-7.19 (m, 2H), 7.03-6.89 (m, 2H), 5.85 (s, 0.6H), 5.68 (s, 0.4H), 4.18-4.13 (m, 0.6H), 3.87-3.84 (m, 0.4H), 3.79+3.78 (s, 3H), 3.36-3.15 (m, 1H), 2.99-2.93 (m, 1H). MS (ESI) m/z 240 (M+1). Anal. Calcd for $\text{C}_{11}\text{H}_{13}\text{NO}_3\text{S}$: C, 55.21; H, 5.48; N, 5.85; Found: C, 55.51; H, 5.46; N, 5.87.

4.1.4

(4R)-2-(4-methoxyphenyl)thiazolidine-4-carboxylic acid (4) yield 81%. ^1H NMR(300 MHz, DMSO- d_6) δ 7.45-7.35 (m, 2H), 6.93-6.86 (m, 2H), 5.59 (s, 0.5H), 5.44 (s, 0.5H), 4.26-4.22 (m, 0.5H), 3.88-3.83 (m, 0.5H), 3.74+3.73 (s, 3H), 3.38-3.25 (m, 1H), 3.17-3.03 (m, 1H). MS (ESI) m/z 240 (M+1). Anal. Calcd for $\text{C}_{11}\text{H}_{13}\text{NO}_3\text{S}$: C, 55.21; H, 5.48; N, 5.85. Found: C, 55.43; H, 5.50; N, 5.83.

4.1.5

(4R)-2-(3-fluorophenyl)thiazolidine-4-carboxylic acid (5) yield 87%. ^1H NMR(300 MHz, DMSO- d_6) δ 7.42-7.24 (m, 3H), 7.17-7.05 (m, 1H), 5.69 (s, 0.6H),

5.51 (s, 0.4H), 4.20-4.16 (m, 0.6H), 3.92-3.87 (m, 0.4H), 3.37-3.26 (m, 1H), 3.13-3.05 (m, 1H). MS (ESI) m/z 226 (M-1). Anal. Calcd for $\text{C}_{10}\text{H}_{10}\text{FNO}_2\text{S}$: C, 52.85; H, 4.44; N, 6.16; Found: C, 52.66; H, 4.46; N, 6.14.

4.1.6

(4R)-2-(4-fluorophenyl)thiazolidine-4-carboxylic acid (6) yield 82%. ^1H NMR(300 MHz, DMSO- d_6) δ 7.62-7.47 (m, 2H), 7.24-7.14 (m, 2H), 5.68 (s, 0.6H), 5.52 (s, 0.4H), 4.24-4.20 (m, 0.6H), 3.93-3.88 (m, 0.4H), 3.41-3.29 (m, 1H), 3.17-3.07 (m, 1H). MS (ESI) m/z 226 (M-1). Anal. Calcd for $\text{C}_{10}\text{H}_{10}\text{FNO}_2\text{S}$: C, 52.85; H, 4.44; N, 6.16; Found: C, 52.99; H, 4.42; F, 8.36; N, 6.19.

4.1.7

(4R)-2-(2-chlorophenyl)thiazolidine-4-carboxylic acid (7) yield 83%. ^1H NMR(300 MHz, DMSO- d_6) δ 7.84-7.83 (m, 0.3H), 7.58-7.55 (m, 0.8H), 7.45-7.22 (m, 3H), 5.96 (s, 0.7H), 5.77 (s, 0.3H), 4.19-4.15 (m, 0.7H), 4.00-3.95 (m, 0.3H), 3.38-3.22 (m, 1H), 3.16-2.94 (m, 1H). MS (ESI) m/z 242 (M-1). Anal. Calcd for $\text{C}_{10}\text{H}_{10}\text{ClNO}_2\text{S}$: C, 49.28; H, 4.14; N, 5.75; Found: C, 49.46; H, 4.17; N, 5.78.

4.1.8

(4R)-2-(3-chlorophenyl)thiazolidine-4-carboxylic acid (8) yield 81%. ^1H NMR(300 MHz, DMSO- d_6) δ 7.66-7.34 (m, 4H), 5.71 (s, 0.6H), 5.53 (s, 0.4H), 4.20-4.17 (m, 0.6H), 3.94-3.88 (m, 0.4H), 3.39-3.29 (m, 1H), 3.15-3.07 (m, 1H). MS (ESI) m/z 242 (M-1). Anal. Calcd for $\text{C}_{10}\text{H}_{10}\text{ClNO}_2\text{S}$: C, 49.28; H, 4.14; N, 5.75; Found: C, 49.54; H, 4.16; N, 5.77.

4.1.9

(4R)-2-(4-chlorophenyl)thiazolidine-4-carboxylic acid (9) yield 78%. ^1H NMR(300 MHz, DMSO- d_6) δ 7.55-7.53 (m, 1H), 7.46-7.35 (m, 3H), 5.69 (s, 0.6H), 5.50 (s, 0.4H), 4.19-4.15 (m, 0.6H), 3.92-3.86 (m, 0.4H), 3.38-3.26 (m, 1H), 3.13-3.04 (m, 1H). MS (ESI) m/z 242 (M-1). Anal. Calcd for $\text{C}_{10}\text{H}_{10}\text{ClNO}_2\text{S}$: C, 49.28; H, 4.14; N, 5.75; Found: C, 49.60; H, 4.12; N, 5.77.

4.1.10

(4R)-2-(2-bromophenyl)thiazolidine-4-carboxylic acid (10) yield 73%. ^1H NMR(300 MHz, DMSO- d_6) δ 7.84-7.54 (m, 2H), 7.54-7.34 (m, 1H), 7.27-7.14 (m, 1H), 5.90 (s, 0.7H), 5.72 (s, 0.3H), 4.20-4.16 (m, 0.7H), 4.00-3.95 (m, 0.3H), 3.37-3.21 (m, 1H), 3.08-2.93 (m, 1H). MS (ESI) m/z 286 (M-1). Anal. Calcd for $\text{C}_{10}\text{H}_{10}\text{BrNO}_2\text{S}$: C, 41.68; H, 3.50; N, 4.86; Found: C, 41.87; H, 3.48; N, 4.88.

4.1.11

(4R)-2-(4-bromophenyl)thiazolidine-4-carboxylic acid (11) yield 87%. ^1H NMR(300 MHz, DMSO- d_6) δ 7.58-7.38 (m, 4H), 5.68 (s, 0.6H), 5.50 (s, 0.4H), 4.19-4.15 (m, 0.6H), 3.93-3.88 (m, 0.4H), 3.39-3.35

(m, 1H), 3.14-3.035 (m, 1H). MS (ESI) m/z 286 (M-1). Anal. Calcd for $C_{10}H_{10}BrNO_2S$: C, 41.68; H, 3.50; N, 4.86. Found: C, 41.51; H, 3.52; N, 4.88.

4.1.12

(4R)-2-(5-fluoro-2-hydroxyphenyl)thiazolidine-4-carboxylic acid (12) yield 84%. 1H NMR(300 MHz, DMSO- d_6) δ 9.89 (b, 0.6H), 7.32-7.27 (m, 0.4H), 7.16-7.12 (m, 0.6H), 7.01-6.87 (m, 1H), 6.84-6.75 (m, 1H), 5.84 (s, 0.6H), 5.66 (s, 0.4H), 4.22-4.18 (m, 0.6H), 3.90-3.85 (m, 0.4H), 3.26-3.260 (m, 1H), 3.05-2.98 (m, 1H). MS (ESI) m/z 242 (M-1). Anal. Calcd for $C_{10}H_{10}FNO_3S$: C, 49.37; H, 4.14; N, 5.76. Found: C, 49.56; H, 4.12; N, 5.74.

General Procedure for the Preparation of TBTCA derivatives 13-24. A mixture of TCA (1.0 mmol) and appropriate NaOH (10%, 1.0 mmol) in dioxane (25 mL) was stirred at ice-water temperature for 2 h. BOC₂O (1.0 mmol) was added and stirred at ice-water temperature for 1 h and then room temperature for 5 h. Most of Solvent was extracted and appropriate amount of water was added to adjust to neutral pH values. Ethyl acetate was added and extracted (50 mL \times 3), and washed with appropriate saturated aqueous solution of common salt, and dried with anhydrous magnesium sulphate. Solvent was extracted to dry to obtain whiter solids 13-24.

4.1.13

(2R,4R)-3-(tert-butoxycarbonyl)-2-phenylthiazolidine-4-carboxylic acid (13) yield 78%. 1H NMR(300 MHz, DMSO- d_6 +CDCl₃) δ 7.56-7.53 (d, 2H), 7.24-7.14 (m, 3H), 6.04+5.85 (2s, 1H), 4.75-4.57 (d, 1H), 3.23-3.16 (m, 2H), 1.34+1.10 (2s, 9H). MS (ESI) m/z 308 (M-1). Anal. Calcd for $C_{15}H_{19}NO_4S$: C, 58.23; H, 6.19; N, 4.53. Found: C, 58.05; H, 6.15; N, 4.57.

4.1.14

(2R,4R)-3-(tert-butoxycarbonyl)-2-(4-hydroxyphenyl)thiazolidine-4-carboxylic acid (14) yield 76%. 1H NMR(300 MHz, DMSO- d_6) δ 9.35 (b, 1H), 7.42-7.39 (d, 2H), 6.68-6.65 (d, 2H), 6.01+5.84 (2s, 1H), 4.67-4.51 (m, 1H), 3.44-3.37 (m, 1H), 3.15-3.05 (m, 1H), 1.34+1.12 (2s, 9H). MS (ESI) m/z 324 (M-1). Anal. Calcd for $C_{15}H_{19}NO_5S$: C, 55.37; H, 5.89; N, 4.30. Found: C, 55.62; H, 6.85; N, 4.32.

4.1.15

(2R,4R)-3-(tert-butoxycarbonyl)-2-(2-methoxyphenyl)thiazolidine-4-carboxylic acid (15) yield 84%. 1H NMR(300 MHz, CDCl₃+TMS) δ 7.83-7.60 (m, 1H), 7.277 (m, 1H), 7.26-7.23 (m, 1H), 6.98-6.85 (m, 1H), 6.38+6.29 (2s, 1H), 4.84-4.71 (m, 1H), 3.86 (s, 3H), 3.40-3.26 (m, 2H), 1.42+1.23 (2s, 9H). MS (ESI) m/z 338 (M-1). Anal. Calcd for $C_{16}H_{21}NO_5S$: C, 56.62; H, 6.24; N, 4.13; Found: C, 56.85; H, 6.22; N, 4.15.

4.1.16

(2R,4R)-3-(tert-butoxycarbonyl)-2-(4-methoxyphenyl)thiazolidine-4-carboxylic acid (16) yield 80%. 1H NMR(300 MHz, CD₂Cl₂) δ 7.45-7.44 (d, 2H),

6.85-6.84 (d, 2H), 5.95 (s, 1H), 4.83 (s, 1H), 3.77 (s, 3H), 3.38-3.31 (m, 2H), 1.27 (s, 9H). MS (ESI) m/z 338 (M-1). Anal. Calcd for $C_{16}H_{21}NO_5S$: C, 56.62; H, 6.24; N, 4.13. Found: C, 56.90; H, 6.21; N, 4.17.

4.1.17

(2R,4R)-3-(tert-butoxycarbonyl)-2-(3-fluorophenyl)thiazolidine-4-carboxylic acid (17) yield 77%. 1H NMR(300 MHz, DMSO- d_6) δ 7.64-7.57 (m, 1H), 7.43-7.31 (m, 2H), 7.10,-7.05 (m, 1H), 6.13+5.97 (2s, 1H), 4.72-4.52 (m, 1H), 3.49-3.43 (m, 1H), 3.20-3.03 (m, 1H), 1.35+1.12 (2s, 9H). MS (ESI) m/z 326 (M-1). Anal. Calcd for $C_{15}H_{18}FNO_4S$: C, 55.03; H, 5.54; N, 4.28; Found: C, 55.35; H, 5.56; N, 4.26.

4.1.18

(2R,4R)-3-(tert-butoxycarbonyl)-2-(4-fluorophenyl)thiazolidine-4-carboxylic acid (18) yield 75%. 1H NMR(300 MHz, CD₂Cl₂) δ 8.80 (bs, 1H), 7.59 (s, 2H), 7.04 (t, 2H), 5.96 (s, 1H), 4.94 (s, 1H), 3.37 (s, 1H), 1.25 (s, 9H). MS (ESI) m/z 326 (M-1). Anal. Calcd for $C_{15}H_{18}FNO_4S$: C, 55.03; H, 5.54; N, 4.28; Found: C, 55.33; H, 5.52; N, 4.30.

4.1.19

(2R,4R)-3-(tert-butoxycarbonyl)-2-(2-chlorophenyl)thiazolidine-4-carboxylic acid (19) yield 80%. 1H NMR(300 MHz, CD₂Cl₂) δ 8.29 (b, 1H), 7.32-7.29 (m, 2H), 7.22-7.16 (m, 2H), 6.26 (s, 1H), 4.78-4.77 (m, 1H), 3.34-3.33 (m, 2H), 1.21 (s, 9H). MS (ESI) m/z 342 (M-1). Anal. Calcd for $C_{15}H_{18}ClNO_4S$: C, 52.40; H, 5.28; N, 4.07; Found: C, 52.40; H, 5.28; N, 4.07.

4.1.20

(2R,4R)-3-(tert-butoxycarbonyl)-2-(3-chlorophenyl)thiazolidine-4-carboxylic acid (20) yield 81%. 1H NMR(300 MHz, DMSO- d_6) δ 13.12 (b, 1H), 7.83-7.79 (d, 1H), 7.59-7.57 (d, 1H), 7.39-7.34 (t, 2H), 6.14+5.98 (2s, 1H), 4.75-4.56 (m, 1H), 3.52-3.46 (m, 1H), 3.22-3.05 (m, 1H), 1.38-1.14 (2s, 9H). MS (ESI) m/z 342 (M-1). Anal. Calcd for $C_{15}H_{18}ClNO_4S$: C, 52.40; H, 5.28; N, 4.07; Found: C, 52.63; H, 5.26; N, 4.09.

4.1.21

(2R,4R)-3-(tert-butoxycarbonyl)-2-(4-chlorophenyl)thiazolidine-4-carboxylic acid (21) yield 73%. 1H NMR(300 MHz, DMSO- d_6) δ 13.08 (b, 1H), 7.67-7.64 (d, 2H), 7.39-7.37 (d, 2H), 6.11+5.96 (2s, 1H), 4.71-4.56 (m, 1H), 3.49-3.43 (m, 1H), 3.36 (m, 1H), 3.17-3.03 (m, 1H), 1.34+1.12 (2s, 9H). MS (ESI) m/z 342 (M-1). Anal. Calcd for $C_{15}H_{18}ClNO_4S$: C, 52.40; H, 5.28; N, 4.07; Found: C, 52.16; H, 5.30; N, 4.05.

4.1.22

(2R,4R)-2-(2-bromophenyl)-3-(tert-butoxycarbonyl)thiazolidine-4-carboxylic acid (22) yield 84%. 1H NMR(300 MHz, DMSO- d_6) δ 13.19 (b, 0.5H), 8.24-8.15 (m, 1H), 7.63-7.56 (m, 1H), 7.40-7.39 (m, 1H), 7.24-7.19 (m, 1H), 6.12 (s, 1H), 4.69-4.52 (m, 1H), 3.54-3.44 (m, 1H), 3.18-2.98 (m, 1H), 1.35+1.10

(2s, 9H). MS (ESI) m/z 386 (M-1). Anal. Calcd for $C_{15}H_{18}BrNO_4S$: C, 46.40; H, 4.67; N, 3.61; Found: C, 46.66; H, 4.69; N, 3.59.

4.1.23

(2R,4R)-2-(4-bromophenyl)-3-(tert-butoxycarbonyl)thiazolidine-4-carboxylic acid (23) yield 78%. 1H NMR(300 MHz, DMSO- d_6) δ 13.07 (b, 0.5H), 7.60-7.58 (d, 2H), 7.52-7.50 (d, 2H), 6.09+5.95 (2s, 1H), 4.70-4.54 (m, 1H), 3.48-3.42 (m, 1H), 3.17-3.03 (m, 1H), 1.34+1.12 (2s, 9H). MS (ESI) m/z 386 (M-1). Anal. Calcd for $C_{15}H_{18}BrNO_4S$: C, 46.40; H, 4.67; N, 3.61. Found: C, 46.72; H, 4.49; N, 3.66.

4.1.24

(2R,4R)-3-(tert-butoxycarbonyl)-2-(5-fluoro-2-hydroxyphenyl)thiazolidine-4-carboxylic acid (24) yield 75%. 1H NMR(300 MHz, DMSO- d_6) δ 7.80-7.76 (m, 1H), 6.91-6.84 (m, 1H), 6.76 (m, 1H), 6.08 (s, 1H), 4.61-4.45 (m, 1H), 3.45-3.39 (m, 1H), 3.11-2.96 (m, 1H), 1.35+1.15 (2s, 9H). MS (ESI) m/z 342 (M-1). Anal. Calcd for $C_{15}H_{18}FNO_5S$: C, 52.47; H, 5.28; N, 4.08. Found: C, 52.11; H, 5.25; N, 4.12.

4.2 Crystallographic studies

X-ray single-crystal diffraction data for '2R, 4R' isomer of compounds **13**, **15**, **21** and **22** were collected on a Nonius CAD4 diffractometer equipped with graphite-monochromatized MoK α ($\lambda = 0.71073$ Å) radiation. The program CAD4 software was used for data collection and cell refinement. Data reduction was solved by XCAD4 program. Structure was solved by direct methods using the SHELXS program of the SHELXTL package and refined by full-matrix least-squares methods with SHELXL¹⁹. All non-hydrogen atoms of '2R, 4R' isomer of compounds **13**, **15**, **21** and **22** were refined with anisotropic thermal parameters. All hydrogen atoms were placed in geometrically idealized positions and constrained to ride on their parent atoms.

4.3 In vitro antibacterial activity

The antibacterial activity of the synthesized compounds was tested against Gram-positive bacteria (*B. subtilis* and *S. aureus*) and Gram-negative bacteria (*P. aeruginosa* and *E. coli*) using MH medium (Mueller-Hinton medium: casein hydrolysate 17.5 g, soluble starch 1.5 g, beef extract 1000 mL). The IC₅₀s of the tested compounds were determined by a colorimetric method using the dye MTT. A stock solution of the synthesized compound (50 μ g/mL) in DMSO was prepared and graded quantities of the tested compounds were incorporated in specified quantity of sterilized liquid medium (MH medium for antibacterial activity). A specified quantity of the medium containing the compound was poured into microtitration plates. Suspension of the microorganism was prepared to contain approximately 10⁵ cfu/mL

and applied to microtitration plates with serially diluted compounds in DMSO to be tested and incubated at 37 °C for 24 h. After the IC₅₀s were visually determined on each of the microtitration plates, 50 mL of PBS (phosphate buffered saline 0.01 mol/L, pH 7.4, Na₂HPO₄·12H₂O (2.9 g), KH₂PO₄ (0.2 g), NaCl (8.0 g), KCl (0.2 g), distilled water (1000 mL) containing 2 mg of MTT/mL was added to each well. Incubation was continued at room temperature for 4–5 h. The content of each well was removed, and 100 mL of isopropanol containing 5% 1 mol/L HCl was added to extract the dye. After 12 h of incubation at room temperature, the optical density (OD) was measured with a microplate reader at 570 nm. The observed IC₅₀s are presented in Table 4.

Acknowledgments

This work was supported by the National Natural Science Foundation of China (No. 21202153) and Foundation of Zhejiang Educational Committee (No. Y201223263). We also thank Dr. Zhe Li (Department of Chemistry, Tsinghua University, Beijing) for the help of the theoretical model calculation.

Notes and references

- H. Pellissier, Recent developments in dynamic kinetic resolution *Tetrahedron*, 2008, 64, 1563-1601.
- O. Pamies, J. E. Backvall, Chemoenzymatic dynamic kinetic resolution. *Trends Biotechnol.*, 2004, 22, 130-135.
- F. F. Huerta, Y. R. S. Laxmi and J. E. Backvall, Dynamic Kinetic Resolution of α -Hydroxy Acid Esters. *Org Lett*, 2000, 2, 1037-1040.
- A. Berkessel, F. Cleemann, S. Mukherjee, T. N. Muller and J. Lex, Bifunktionale Organokatalysatoren auf Harnstoff-Basis für die effiziente dynamische kinetische Racemattrennung von Azlactonen, *Angew Chem*, 2005, 117, 659. Highly Efficient Dynamic Kinetic Resolution of Azlactones by Urea-Based Bifunctional Organocatalysts. *Angew Chem Int Ed*, 2005, 44, 807-811.
- V. Chan, J.G. Kim, C. Jimeno, P.J. Carroll and P. J. Walsh, Dynamic Kinetic Resolution of Atropisomeric Amides. *Org Lett*, 2004, 6, 2051-2053.
- S. L. You and J. W. Kelly, Highly Efficient Biomimetic Total Synthesis and Structural Verification of Bistratamides E and J from *Lissoclinum bistratum*. *Chem Eur J*, 2004, 10, 71-75.
- L. Szilagyi and Z. Gyorgydeak, Comments on the putative stereoselectivity in cysteine-aldehyde reactions. Selective C(2) inversion and C(4) epimerization in thiazolidine-4-carboxylic acids. *J Am Chem Soc*, 1979, 101, 427-432.
- R.G. Kallen, Mechanism of reactions involving Schiff base intermediates. Thiazolidine formation from L-cysteine and formaldehyde. *J Am Chem Soc*, 1971, 93, 6236-6248.
- M. Seki, M. Hatsuda, Y. Mori, S. I. Yoshida, S. I. Yamada and T. Shimizu, A Practical Synthesis of (+)-Biotin from L-Cysteine. *Chem Eur J*, 2004, 10, 6102-6110.

- 10 A. Wagner, R. Flaig, B. Dittrich, H. Schmidt, T. Koritsánszky and P. Luger, Charge Density and Experimental Electrostatic Potentials of Two Penicillin Derivatives. *Chem Eur J*, 2004, 10, 2977-2982.
- 11 A. Serganov, A. Polonskaia, A. T. Phan, R. R. Breaker and D. J. Patel, Structural basis for gene regulation by a thiamine pyrophosphate-sensing riboswitch. *Nature*, 2006, 441, 1167-1171.
- 12 V. Sriramurthy, G. A. Barcan and O. Kwon, Bisphosphine-Catalyzed Mixed Double-Michael Reactions: Asymmetric Synthesis of Oxazolidines, Thiazolidines, and Pyrrolidines. *J Am Chem Soc*, 2007, 129, 12928-12929.
- 13 V. Gududuru, E. Hurh, J. T. Dalton and D. D. Miller, Discovery of 2-Arylthiazolidine-4-carboxylic Acid Amides as a New Class of Cytotoxic Agents for Prostate Cancer. *J Med Chem*, 2005, 48, 2584-2588.
- 14 A. Traff, K. Bogar, M. Warner and J. E. Backvall, Highly Efficient Route for Enantioselective Preparation of Chlorohydrins via Dynamic Kinetic Resolution. *Org Lett*, 2008, 10, 4807-4810.
- 15 A. Klapars, K. R. Campos, J. H. Waldman, D. Zewge, P. G. Dormer and C. Y. Chen, Enantioselective Pd-Catalyzed α -Arylation of *N*-Boc-Pyrrolidine: The Key to an Efficient and Practical Synthesis of a Glucokinase Activator. *J Org Chem*, 2008, 73, 4986-4993.
- 16 Z. C. Song, G. Y. Ma, P. C. Lv, H. Q. Li, Z. P. Xiao and H. L. Zhu, Synthesis, structure and structure-activity relationship analysis of 3-tert-butoxycarbonyl-2-arylthiazolidine-4-carboxylic acid derivatives as potential antibacterial agents. *Eur J Med Chem*, 2009, 44, 3903-3908.
- 17 M. Seki, Y. Mori, M. Hatsuda and S. Yamada, A Novel Synthesis of (+)-Biotin from *L*-Cysteine. *J Org Chem*, 2002, 67, 5527-5536.
- 18 M. E. F. Braibante, H. S. Braibante, E.R. Costenaro, The Use of Curtius Rearrangement in the Synthesis of 4-Aminothiazolidines. *Synthesis*, 1999, 6, 943-946.
- 19 G. M. Sheldrick, SHELXTL-97, Program for Crystal Structure Solution and Refinement; University of Go'ttingen: Go'ttingen, Germany, 1997.
- 20 H. D. Flack, On enantiomorph-polarity estimation. *Acta Crystallogr, Sect A*, 1983, 39, 876-881.
- 21 J. Zhang, S. Chen, T. Wu, P. Feng and X. Bu Homochiral Crystallization of Microporous Framework Materials from Achiral Precursors by Chiral Catalysis. *J Am Chem Soc*, 2008, 130, 12882-12883.
- 22 D. E. Williams, J. Davies, B. O. Patrick, H. Bottrill, T. Tarling, M. Roberge, R. J. Andersen and A. G. Cladoniamides, Tryptophan-Derived Alkaloids Produced in Culture by *Streptomyces uncialis*. *Org Lett*, 2008, 10, 3501-3504.
- 23 M. J. Frisch, G. W. Trucks, H. B. Schlegel, G. E. Scuseria, M. A. Robb, J. R. Cheeseman, J. A. Montgomery, Jr., T. Vreven, K. N. Kudin, J. C. Burant, J. M. Millam, S. S. Iyengar, J. Tomasi, V. Barone, B. Mennucci, M. Cossi, G. Scalmani, N. Rega, G. A. Petersson, H. Nakatsuji, M. Hada, M. Ehara, K. Toyota, R. Fukuda, J. Hasegawa, M. Ishida, T. Nakajima, Y. Honda, O. Kitao, H. Nakai, M. Klene, X. Li, J. E. Knox, H. P. Hratchian, J. B. Cross, V. Bakken, C. Adamo, J. Jaramillo, R. Gomperts, R. E. Stratmann, O. Yazyev, A. J. Austin, R. Cammi, C. Pomelli, J. W. Ochterski, P. Y. Ayala, K. Morokuma, G. A. Voth, P. Salvador, J. J. Dannenberg, V. G. Zakrzewski, S. Dapprich, A. D. Daniels, M. C. Strain, O. Farkas, D. K. Malick, A. D. Rabuck, K. Raghavachari, J. B. Foresman, J. V. Ortiz, Q. Cui, A. G. Baboul, S. Clifford, J. Cioslowski, B. B. Stefanov, G. Liu, A. Liashenko, P. Piskorz, I. Komaromi, R. L. Martin, D. J. Fox, T. Keith, M. A. Al-Laham, C. Y. Peng, A. Nanayakkara, M. Challacombe, P. M. W. Gill, B. Johnson, W. Chen, M. W. Wong, C. Gonzalez, and J. A. Pople, Gaussian 03, revision C02, Gaussian, Inc: Wallingford, CT, 2004.
- 24 A. D. Becke, Density-functional thermochemistry. III. The role of exact exchange. *J Chem Phys*, 1993, 98, 5648-5652.
- 25 C. Lee, W. Yang and R. G. Parr, Development of the Colle-Salvetti correlation-energy formula into a functional of the electron density. *Phys Rev B*, 1988, 37, 785-789.
- 26 S. Miertuš, E. Scrocco and J. Tomasi, Electrostatic interaction of a solute with a continuum - a direct utilization of abinitio molecular potentials for the prevision of solvent effects. *Chem Phys*, 1981, 55, 117-129.